Research Article
Hepatic and Biliary Cancer

JOURNAL OF HEPATOLOGY

Mitochondrial oxidative metabolism contributes to a cancer stem cell phenotype in cholangiocarcinoma

Chiara Raggi[1,*], Maria Letizia Taddei[1], Elena Sacco[2,3], Nadia Navari[1], Margherita Correnti[4], Benedetta Piombanti[1], Mirella Pastore[1], Claudia Campani[1], Erica Pranzini[1], Jessica Iorio[1], Giulia Lori[1], Tiziano Lottini[1], Clelia Peano[5,6], Javier Cibella[5], Monika Lewinska[7], Jesper B. Andersen[7], Luca di Tommaso[8,9], Luca Viganò[9,10], Giovanni Di Maira[1], Stefania Madiai[1], Matteo Ramazzotti[11], Ivan Orlandi[2,3], Annarosa Arcangeli[1], Paola Chiarugi[11,12], Fabio Marra[1,12,*]

[1]*Department of Experimental and Clinical Medicine, University of Florence, Florence, Italy;* [2]*SYSBIO, Centre of Systems Biology, Milan, Italy;* [3]*Department of Biotechnology and Biosciences, University of Milano-Bicocca, Milan, Italy;* [4]*Center for Autoimmune Liver Diseases, Humanitas Clinical and Research Center, Rozzano, Italy;* [5]*Genomic Unit, IRCCS, Humanitas Clinical and Research Center, Rozzano, Italy;* [6]*Institute of Genetic and Biomedical Research, UoS Milan, National Research Council, Rozzano, Italy;* [7]*Biotech Research and Innovation Centre, University of Copenhagen, Copenhagen, Denmark;* [8]*Department of Pathology, Humanitas Clinical and Research Center, Rozzano, Italy;* [9]*Department of Biomedical Sciences, Humanitas University, Rozzano, Italy;* [10]*Department of Hepatobiliary Surgery, Humanitas Clinical and Research Center, Rozzano, Italy;* [11]*Department of Experimental and Clinical Biomedical Sciences, University of Florence, Florence, Italy;* [12]*Excellence Center for Research, Transfer and High Education DenoTHE, Florence, Italy*

Background & Aims: Little is known about the metabolic regulation of cancer stem cells (CSCs) in cholangiocarcinoma (CCA). We analyzed whether mitochondrial-dependent metabolism and related signaling pathways contribute to stemness in CCA.

Methods: The stem-like subset was enriched by sphere culture (SPH) in human intrahepatic CCA cells (HUCCT1 and CCLP1) and compared to cells cultured in monolayer. Extracellular flux analysis was examined by Seahorse technology and high-resolution respirometry. In patients with CCA, expression of factors related to mitochondrial metabolism was analyzed for possible correlation with clinical parameters.

Results: Metabolic analyses revealed a more efficient respiratory phenotype in CCA-SPH than in monolayers, due to mitochondrial oxidative phosphorylation. CCA-SPH showed high mitochondrial membrane potential and elevated mitochondrial mass, and overexpressed peroxisome proliferator-activated receptor gamma coactivator (PGC)-1α, a master regulator of mitochondrial biogenesis. Targeting mitochondrial complex I in CCA-SPH using metformin, or PGC-1α silencing or pharmacologic inhibition (SR-18292), impaired spherogenicity and expression of markers related to the CSC phenotype, pluripotency, and epithelial-mesenchymal transition. In mice with tumor xenografts generated by injection of CCA-SPH, administration of metformin or SR-18292 significantly reduced tumor growth and determined a phenotype more similar to tumors originated from cells grown in monolayer. In patients with CCA, expression of PGC-1α correlated with expression of mitochondrial complex II and of stem-like genes. Patients with higher PGC-1α expression by immunostaining had lower overall and progression-free survival, increased angioinvasion and faster recurrence. In GSEA analysis, patients with CCA and high levels of mitochondrial complex II had shorter overall survival and time to recurrence.

Conclusions: The CCA stem-subset has a more efficient respiratory phenotype and depends on mitochondrial oxidative metabolism and PGC-1α to maintain CSC features.

Lay summary: The growth of many cancers is sustained by a specific type of cells with more embryonic characteristics, termed 'cancer stem cells'. These cells have been described in cholangiocarcinoma, a type of liver cancer with poor prognosis and limited therapeutic approaches. We demonstrate that cancer stem cells in cholangiocarcinoma have different metabolic features, and use mitochondria, an organelle located within the cells, as the major source of energy. We also identify PGC-1α, a molecule which regulates the biology of mitochondria, as a possible new target to be explored for developing new treatments for cholangiocarcinoma.

Introduction

Cholangiocarcinoma (CCA) represents the second most common form of primary liver cancer,[1–3] with limited therapeutic approaches.[4,5] As a result, the prognosis is still dismal with a 5-year survival lower than 20%.[4,5] These features make CCA a top priority in the field of cancer research.[4,5] The hypothesis of the existence of a cancer stem cell (CSC) population was recently validated by the identification of a subpopulation of self-renewing cells that gives rise to maturational lineages with a hierarchical organization, which divide symmetrically and asymmetrically to generate the tumor mass.[6–14] CSCs, also referred to as tumor-initiating cells or tumor-propagating cells,

Keywords: HUCCT1; CCLP1; OXPHOS; PGC-1α; SR-18292.
Received 22 March 2020; received in revised form 18 December 2020; accepted 24 December 2020; available online 21 January 2021

* Corresponding authors. Addresses: Dipartimento di Medicina Sperimentale e Clinica, Largo Brambilla 3, I50134 Florence, Italy; (F. Marra), or Dipartimento di Medicina Sperimentale e Clinica, Largo Brambilla 3, I50134 Florence, Italy; (C. Raggi).
E-mail addresses: fabio.marra@unifi.it (F. Marra), chiara.raggi@unifi.it (C. Raggi).

https://doi.org/10.1016/j.jhep.2020.12.031

are tumorigenic, metastatic, resistant to chemo-and radiation therapy and are responsible for tumor recurrence.[8–14] In the past years, alongside others, we have highlighted the biology of CSCs in CCA,[15–17] identifying them as a major therapeutic target.[8–14]

Recent studies have identified oxidative phosphorylation (OXPHOS) in cancer cell mitochondria as a novel approach to decrease tumor growth and chemotherapy-resistance in CCA.[18,19] Although mitochondrial metabolism may provide new therapeutic targets, metabolic reprogramming in CCA is underestimated. In addition, the metabolic profiles of CSCs may be an important factor for stemness maintenance, contributing to failure of anticancer treatments,[20,21] but little is known regarding this topic in human CCA. Herein, we show that mitochondrial oxidative metabolism contributes to maintain stemness features in CCA, conferring *in vivo* tumorigenic capacity and drug resistance.

Materials and methods

For details regarding the materials and methods used, please refer to the CTAT table and supplementary information.

Results

The CCA stem-like subset is characterized by mitochondrial oxidative metabolism

We recently identified a functional CSC-subset in human CCA using a 3D sphere culture model.[13] We first characterized if stemness features were associated with differences in energy metabolism, comparing sphere cultures (SPH) generated from HUCCT1 or CCLP1 cells with the same cells grown in monolayer cultures (MON). Bioenergetics parameters were analyzed by Seahorse technology, which enables the simultaneous measurement of oxygen consumption rate (OCR) and extracellular acidification rate (ECAR), key indicators of mitochondrial respiration and glycolysis, respectively, in live cells. Seahorse mitostress, which provides respiratory parameters, showed that SPH have higher OCR than MON both in basal and in FCCP (carbonyl cyanide-4-(trifluoromethoxy) phenylhydrazone)-uncoupled conditions (Fig. 1A; Fig. S1A-B). In addition, the response to oligomycin A, which accounts for non-phosphorylating respiration, indicated that OCR, even enhanced, in SPH cells is coupled to ATP production similarly, or only weakly less, to that of MON cells (see values of the coupling efficiency of oxidative phosphorylation). These data indicate that SPH show increased mitochondrial respiration coupled to ATP production, likely related to a potentiated respiratory machinery, in both HUCCT1 and CCLP1 cells. Seahorse analysis requires forced adhesion of SPH to perform the assay. Although no significant differences in respiratory capacity of SPH cells forced to adhere on XF plates for as long as 20 hours were observed (data not shown), we aimed to confirm the Seahorse findings with an alternative method, which may be applied to cells in suspension. To do this, we analyzed OCR of SPH maintained in suspension, using a “Clark-type” oxygen electrode. Oxygraph analysis (Fig. 1B) fully confirmed Seahorse data, suggesting that the enhanced mitochondrial respiration of SPH is a property acquired during the adaptation to 3D cell growth, and not an artifact dependent on the analytical methods used.

We next used the Seahorse glycostress protocol to measure glycolytic parameters of MON and SPH of both cell lines. This test (Fig. 1C, Fig. S1) showed that basal and oligomycin-accelerated ECAR are similar in SPH and MON, indicating limited, if any, differences in glycolytic capacity and reserve. Because SPH and MON are grown in media of different composition, we aimed to rule out that these differences could modify metabolic parameters independently of the "stemness" status of the cells. When MON cells were grown in SPH culture medium for 5 days, no variations in OCR parameters or in the expression of stemness-related genes were observed, indicating that metabolic differences only depend on 3D culture as a representation of a stem-like state (Fig. S2). Taken together, these results indicate that when HUCCT1 or CCLP1 are grown as spheres, a profound change in energy metabolic profile, with enhanced mitochondrial respiration, is observed (Fig. 1D).

The CCA stem-like subset is more sensitive to interference with mitochondrial function

Since CCA-SPH preferentially rely on OXPHOS, we further evaluated the role of mitochondria in the stem-like compartment. In CCA-SPH a significantly higher mitochondrial membrane potential was measured with MitoTracker Red staining, together with increased mitochondrial mass (MitoTracker Green, Fig. 2A). The peroxisome proliferator-activated receptor gamma coactivator (PGC) family, in particular PGC-1α,[22,23] acts as a master regulator of mitochondrial *de novo* synthesis, and regulates different energy-producing metabolic processes in the liver, including OXPHOS. In CCA-SPH, over-expression of PGC-1α at the protein and mRNA levels (Fig. 2B-C) was observed, providing additional support for a role of mitochondria in cells of the CCA stem-like subset. In contrast, CCA-SPH cells showed reduced glucose uptake (Fig. 2D), together with lower production of lactate, a metabolic product of glycolysis (Fig. 2E). Downregulation of the glycolytic pathway is also indicated by repressed gene expression of the Glut1 transporter (Fig. 2F) as well as of hexokinase II (HKII) and pyruvate kinase M2 (Fig. 2G). Remarkably, gene set-enrichment analysis (GSEA) of RNA-sequencing data confirmed the downregulation of the glycolytic component in CCA-SPH when compared to MON (Fig. 2H). In contrast, no differences in mitochondrial reactive oxygen species levels were observed between MON and SPH, indicating that differences in glycolytic flux are not due to an impairment in mitochondrial functionality (Fig. S3A).

It is well-known that activated AMPK regulates PGC-1α expression.[24] In accordance with high levels of PGC-1α in SPH cells (Fig. 2B-C), the AMP/ATP ratio was higher in SPH than in MON (Fig. S3B), together with increased activation of AMPK signaling, as demonstrated by higher levels of AMPK phosphorylation (Fig. S3C). In other tumors, AMPK activation correlates with epithelial-mesenchymal transition (EMT).[25–27] To establish whether AMPK regulates these processes in CCA-SPH, SPH were treated with compound C, a well-established inhibitor of AMPK phosphorylation[28] (Fig. S3D). Treatment with compound C markedly reduced the expression level of genes implicated in EMT, indicating a contribution of the AMPK pathway in this relevant process associated with malignancy (Fig. S3B).

To provide functional evidence for a role of mitochondria in maintaining the CCA stem-like subset, cell survival was evaluated after treatment with metformin or phenformin, both inhibitors of mitochondrial complex I. SPH were consistently more sensitive to inhibitors of mitochondrial complex I than cells grown in MON (Fig. S4A). Conversely, treatment with 2-deoxy-D-glucose, an antagonist of glucose uptake, had a greater effect on survival of glycolysis-dependent MON (Fig. S4B). Interestingly,

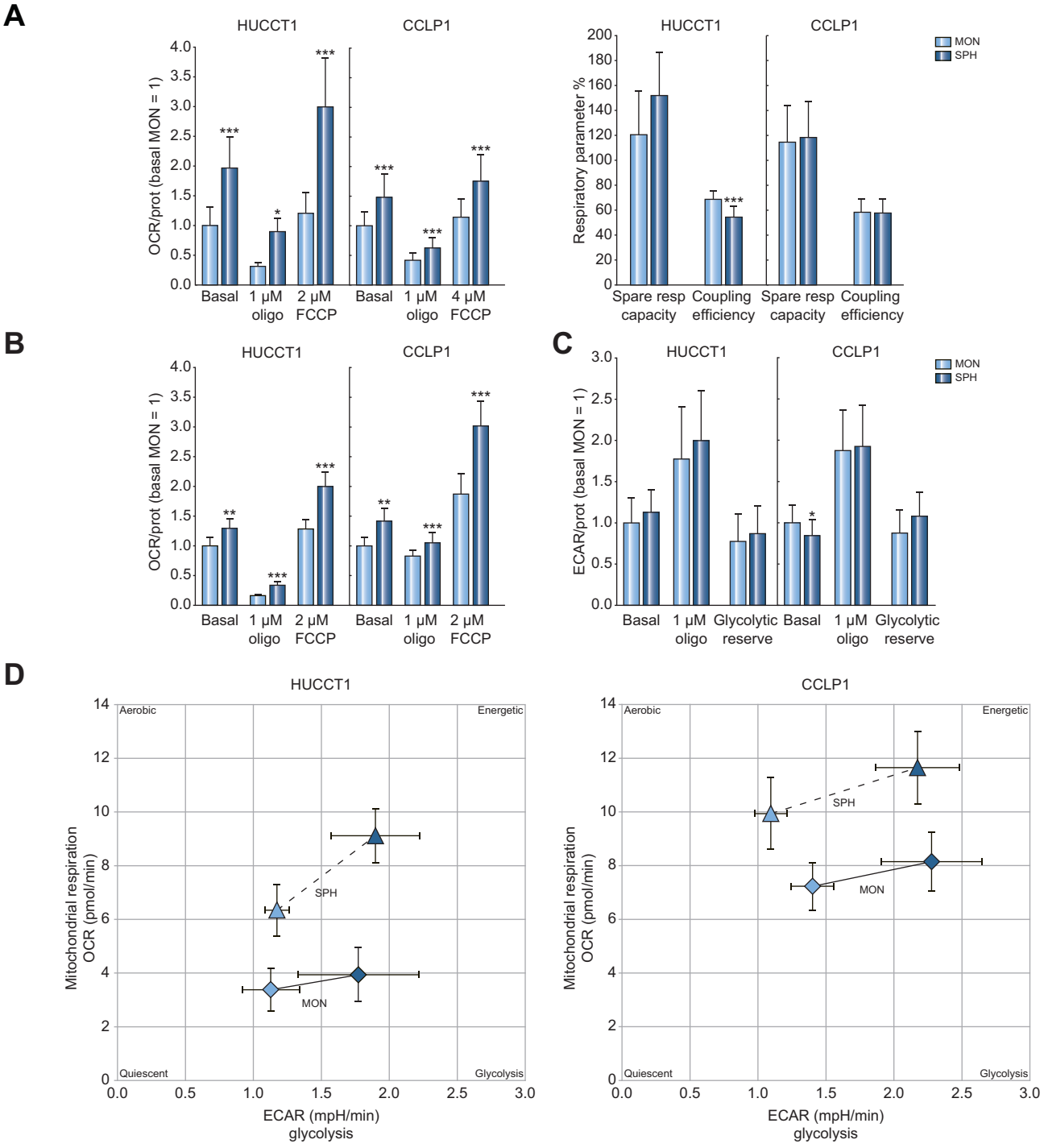

Fig. 1. Metabolic characteristics of CCA cells grown as monolayers or spheres. (A-B) OCRs of HUCCT1 and CCLP1 cells, as assessed by Seahorse mitostress test (A) or oxygraph (B) analysis. Respiratory parameters include basal mitochondrial respiration, response to oligomycin A accounting for non-phosphorylating mitochondrial respiration (oligo), FCCP-uncoupled mitochondrial respiration, spare respiratory capacity and coupling efficiency, calculated as described in the supplementary materials and methods. Data were normalized on basal respiratory parameters in MON. (C) ECAR parameters derived from Seahorse glycostress test analysis, normalized on basal glycolytic parameters of MON. Results are mean ± SD of 2 independent experiments performed on 10 (Seahorse) and 3 (Oxygraph) replicates for each condition (*$p \leq 0.05$, **$p \leq 0.01$, ***$p \leq 0.001$ *vs.* MON by Student's *t* test). (D) Energy phenotype of HUCCT1 and CCLP1 cells grown as MON (diamonds) or SPH (triangles) in basal (empty shapes) or metabolic stress (full shapes) conditions, as described in the supplementary materials and methods. CCA, cholangiocarcinoma; ECAR, extracellular acidification rate; MON, monolayer cultures; OCR, oxygen consumption rate; SPH, sphere cultures.

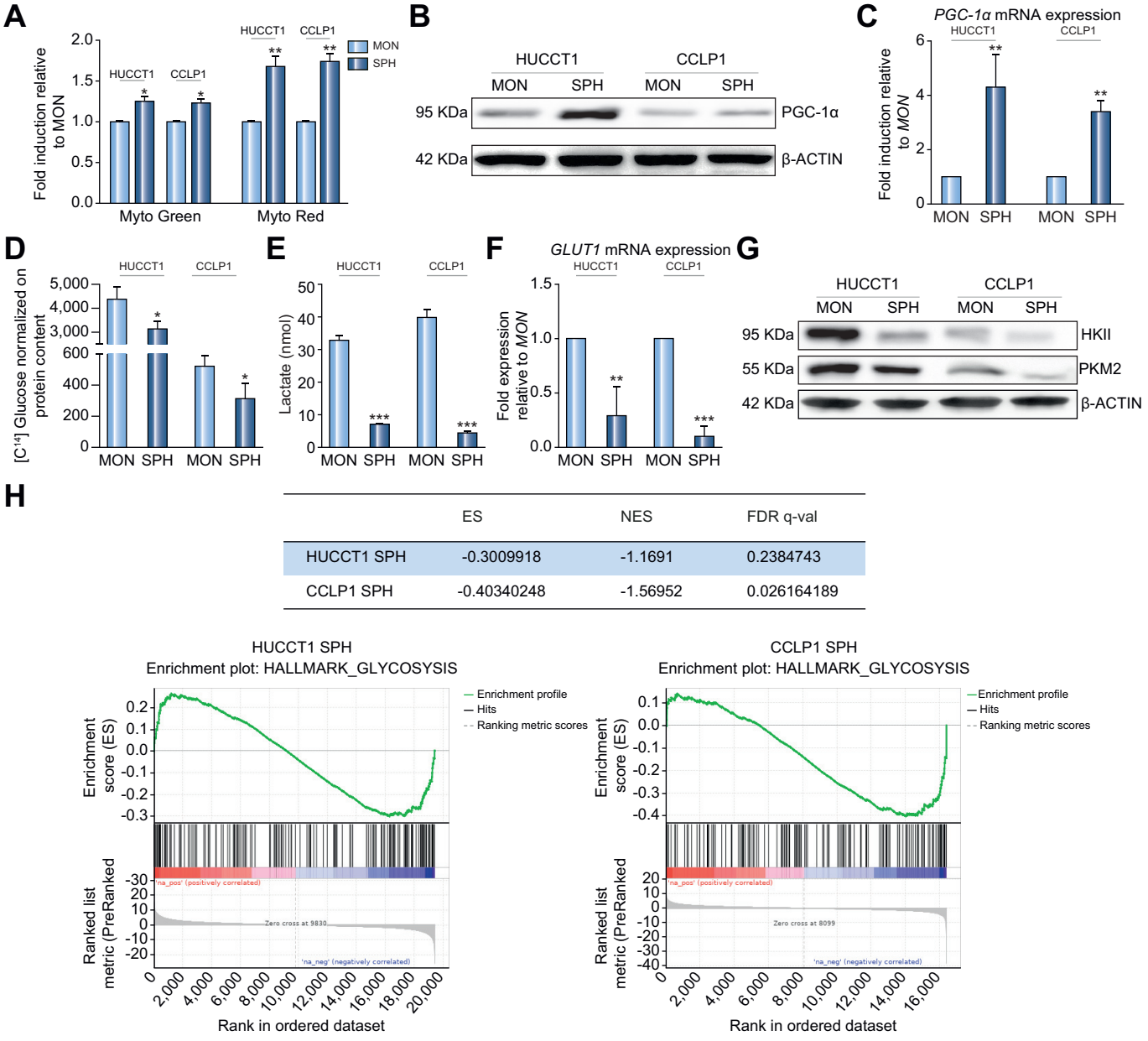

	ES	NES	FDR q-val
HUCCT1 SPH	-0.3009918	-1.1691	0.2384743
CCLP1 SPH	-0.40340248	-1.56952	0.026164189

Fig. 2. Mitochondrial mass and glycolysis are differentially regulated in CCA cells grown as MON or SPH. (A) Mitochondrial mass and membrane potential were measured by FACS. Histograms represent the MFI of the MitoTracker probes normalized to mean MFI of MON. Data are mean ± SEM (n = 3, *$p \leq 0.05$, **$p \leq 0.01$ *vs.* MON by Student's *t* test). (B) Immunoblot of PGC-1α. β-actin immunoblot was performed to ensure equal loading. (C) *PGC-1α* gene expression levels, presented as fold changes normalized to mean expression of MON. GAPDH was used as an internal control. Data are mean ± SEM (n = 3, **$p \leq 0.01$ *vs.* MON by Student's *t* test). (D) [^{14}C]-glucose uptake normalized by total proteins. Data are mean ± SEM (n = 3, *$p \leq 0.05$ *vs.* MON by Student's *t* test). (E) Extracellular lactate levels normalized by protein content. Data are mean ± SEM (n = 3, ***$p \leq 0.001$ *vs.* MON by Student's *t* test). (F) *GLUT1* gene expression levels, presented as in panel C. Mean ± SEM (n = 3, **$p \leq 0.01$, ***$p \leq 0.001$ *vs.* MON by Student's *t* test). (G) Immunoblot of HKII and PKM2, presented as in panel B. (H) Results of a GSEA Pre-ranked analysis on the Glycolysis gene set of the Hallmark MSigDB collection. CCA, cholangiocarcinoma; ES, enrichment score; FDR, false discovery rate; GSEA, gene set-enrichment analysis; MFI, mean fluorescent intensity; MON, monolayer cultures; NES, normalized enrichment score; SPH, sphere cultures.

this effect was less marked, and not statistically significant, in CCLP1 cells, which express lower levels of HKII, and have a lower ability to incorporate glucose. These results reinforce the concept that CCA stem-like cells are more reliant on mitochondrial metabolism than cells in MON, which are more sensitive to the glycolysis pathway.

Exposure to metformin dramatically reduced the expression of molecules related to stemness, self-renewal, pluripotency, drug resistance and EMT in SPH of both CCA cell lines, while virtually no effects were found in MON (Fig. S4C-D). Moreover, metformin reduced activation of the Akt pathway only in SPH (Fig. S4C-D). These data indicate that interfering with mitochondrial respiration affects the stemness component of CCA.

PGC-1α is required to maintain stemness features and pro-angiogenic actions of CCA

Because PGC-1α, a critical regulator of mitochondrial function, is expressed at higher levels in SPH, we tested the effects of genetic

knockdown or pharmacologic inhibition of this molecule on functional characteristics and intracellular signaling of SPH from both CCLP1 and HUCCT1. As expected, PGC-1α depletion (Fig. 3A) impaired mitochondrial mass (Fig. S5A). Although PGC-1α silencing did not affect cell proliferation or apoptosis (Fig. S5B-C), it markedly reduced CCA stem-like properties such as *in vitro* spherogenicity (Fig. 3B, Fig. S5D) and expression of CSC-related genes (Fig. 3C). These functional effects were accompanied by a marked downregulation of signaling pathways relevant for CCA biology in SPH silenced for PGC-1α (Fig. 3D). Similarly, PGC-1α knockdown significantly reduced the ability to invade a basement-membrane-like matrix (Fig. 3E) and to migrate in a Boyden chamber assay (Fig. S5E), key features of highly malignant CCA cells. Furthermore, we found a significant correlation between expression of PGC-1α and that of many stem-like genes in a transcriptomic database of patients with CCA (Fig. 3F).[29]

Angiogenesis is critical to develop and sustain a microenvironment favorable to maintain the properties of CSC, and we

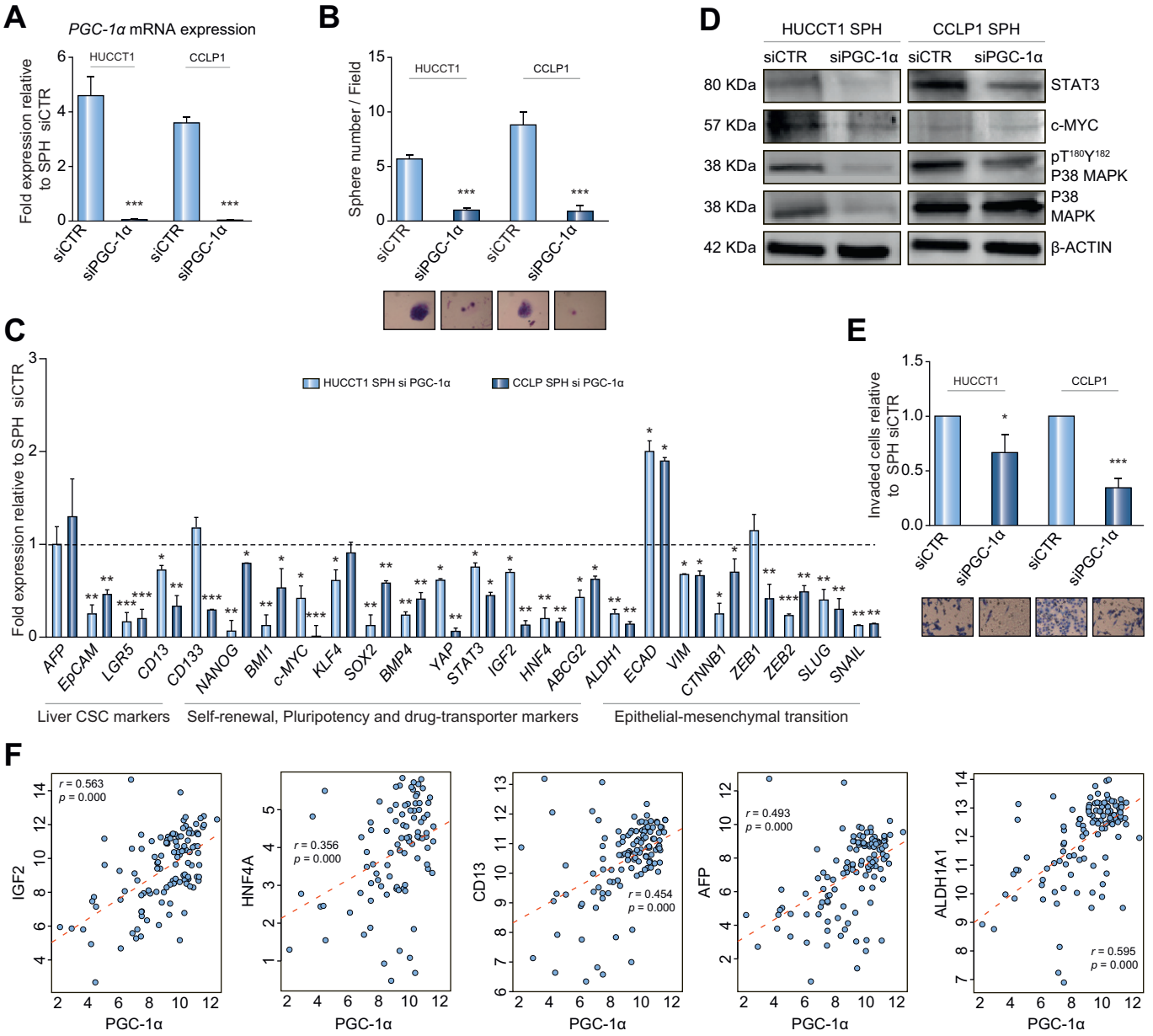

Fig. 3. Effects of PGC-1α silencing in CCA-SPH cells. (A) PGC-1α gene expression levels following siRNA transfection, presented as fold changes normalized to mean expression of siCTR (n = 4, mean ± SEM, ***$p \leq 0.001$ *vs.* siCTR by Student's *t* test). (B) Effects of PGC-1α silencing on CCA sphere-forming efficiency. Mean ± SEM (n = 3, ***$p \leq 0.001$ *vs.* siCTR by Student's *t* test). Representative images of CCA-SPH are shown below the barogram (original magnification 40X, scale bar 10μM). (C) Expression of different genes, expressed as fold changes normalized to mean expression of siCTR sample. Mean ± SEM (n = 3, *$p \leq 0.05$, **$p \leq 0.01$, ***$p \leq 0.001$ *vs.* siCTR by Student's *t* test). Gene groups are indicated at the bottom of the barograms. (D) Immunoblot of different proteins or phosphoproteins following PGC-1α silencing. (E) Invasion of PGC-1α-silenced CCLP1 and HUCCT1 cells was measured in modified Boyden chambers. Mean ± SEM (n = 5, *$p \leq 0.05$, ***$p \leq 0.001$ *vs.* siCTR by Student's *t* test). Representative images of filters are shown below the barograms (original magnification 40x, scale bar 10μM. (F) Scatterplots representing correlations between expression levels of PGC-1α (x-axis) and stem-like genes (y-axis) according to a published microrarray-based study comparing CCA *vs.* surrounding liver (GSE26566[25]). All adjusted (2-tailed) *p* values were <1e-5. CCA, cholangiocarcinoma; MFI, mean fluorescent intensity; SPH, sphere cultures; siPGC-1α, PGC-1α silenced cells; siCTR, silenced control.

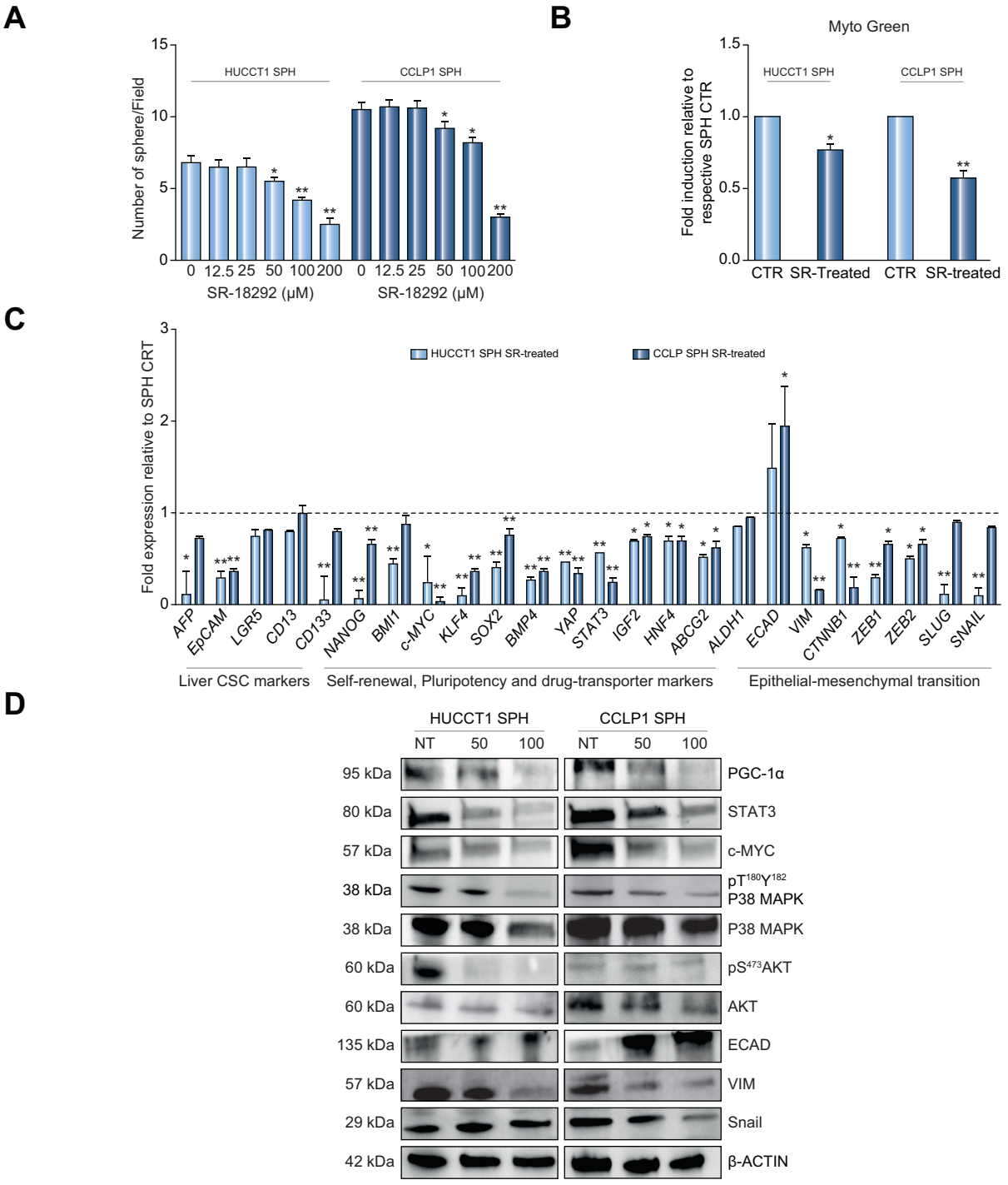

Fig. 4. Effects of the PGC-1α inhibitor SR-18292 in CCA-SPH cells. (A) Sphere-forming efficiency after SR-18292 exposure. Mean ± SEM (n = 3, $^{*}p \leq 0.05$, $^{**}p \leq 0.001$ *vs.* control by Student's *t* test). (B) Mitochondrial mass, measured with MitoTracker Green, as described in Fig. 2A, presented as fold induction normalized to mean MFI of control). Mean ± SEM (n = 3, $^{*}p \leq 0.05$, $^{**}p \leq 0.01$ *vs.* control by Student's *t* test). (C) Expression of different genes, expressed as fold changes normalized to mean expression of control sample) (n = 3). Mean ± SEM ($^{*}p \leq 0.05$, $^{**}p \leq 0.01$ *vs.* CTR by Student's *t* test). (D) Immunoblot of different proteins and phosphoproteins following SR-18292 treatment. CCA, cholangiocarcinoma; MFI, mean fluorescent intensity; SPH, sphere cultures.

previously demonstrated[13] that conditioned medium from CCA-SPH induces a higher angiogenic response than that from MON. In SPH silenced for PGC-1α or treated with metforrmin, vascular endothelial growth factor (VEGF) expression was significantly reduced in both cell lines (Fig. S6A), indicating that the action of PGC-1α is likely to be mediated by mitochondria. As a clinical counterpart, a significant correlation between VEGF and PGC-1α expression was found in a transcriptomic database of patients with CCA (Fig. S6B). To confirm that PGC-1α regulates angiogenesis, we tested the effects of conditioned medium from SPH

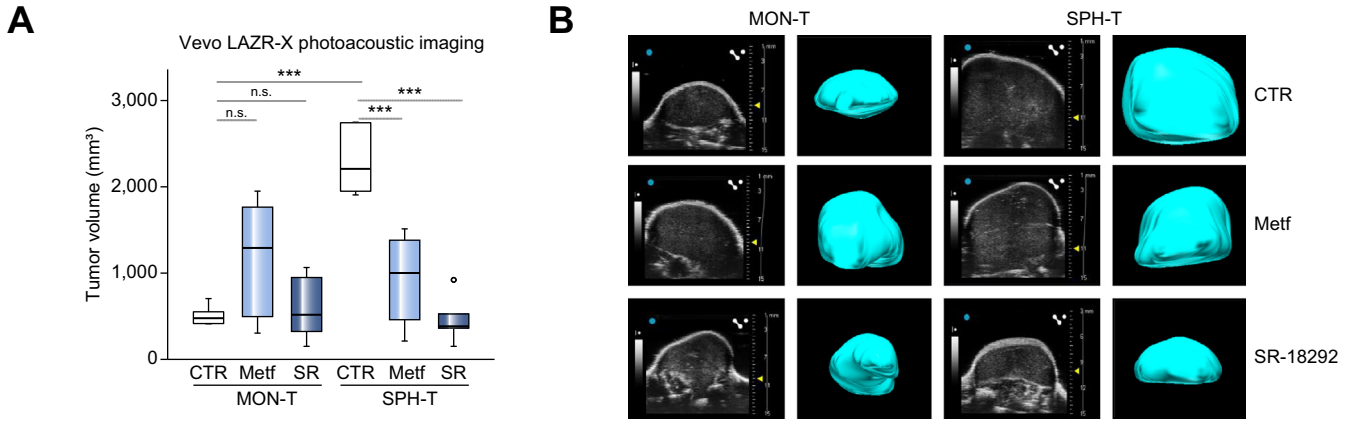

Fig. 5. Effects of metformin and SR-18292 on tumor xenografts. Tumors derived from HUCCT1 cells grown as MON or SPH were obtained by subcutaneous injection in NOD/SCID mice. After 7 days, mice were treated with PBS (CTR), metformin (Metf) or SR-18292 (SR) (n = 6 per group). (A) Analysis of tumor volume by Vevo LAZR-X photoacoustic imaging. The box height represents the interquartile range (Q1–Q3), the line within the box is the median value, the lower and upper whiskers represents the lowest and the highest samples, respectively. Circles in boxplots represent outlier samples (>1.5xIQR). ***p <0.002 or less by Mann-Whitney U test (B) Representative high-resolution ultrasound images of subcutaneous tumors from mice in each group. The cyan 3D regions represent the tumor volume obtained by tracing areas on each 2D B-mode slices from the 3D acquisition. MON, monolayer cultures; SPH, sphere cultures, MON-T, tumors derived from injected monolayer cells; SPH-T, tumors derived by injected sphere cells.

on capillary tube-like formation by human umbilical vein endothelial cells in an angiogenic assay (Fig. S6C-D). As expected, depletion of PGC-1α in SPH drastically reduced the neovascular response in CCA-SPH. Overall, these data show that the CSC microvascular environment is dependent on tumor metabolic activity, regulated by PGC-1α.

To obtain additional information on the potential role of PGC-1α, we employed SR-18292, a selective pharmacological inhibitor which increases PGC-1α acetylation and its inhibition.[30,31] Treatment with SR-18292 reduced PGC-1α levels and mitochondrial mass (Fig. 4A-B), cell viability, expression of Myc and STAT3, and activation of P38MAPK and AKT (Fig. 4C-D). In addition, pharmacologic inhibition of PGC-1α modulated a broad range of genes implicated in maintenance of stemness, self-renewal, and regulation of EMT (Fig. 4C-D). These data identify mitochondrial respiration and PGC-1α as relevant targets in CCA stem-like cells.

To demonstrate that interference with mitochondrial respiration may have an impact on CCA stem-compartment growth *in vivo*, we analyzed the effects of metformin and of SR-18292 on tumors obtained by subcutaneous injection of cells derived from SPH or from cells grown in MON. The growth of xenografts was monitored with a dedicated *in vivo* imaging system (Vevo LAZR-X photoacoustic imaging), which allows 3D-reconstruction and exact calculation of tumor volume (Fig. 5). As expected, 28 days after injection, the volume of tumors derived from SPH were significantly larger than those from MON. Treatment of mice with metformin or SR-18292 did not significantly modify the volume of tumors derived from MON. In contrast, the growth of tumors derived from SPH was significantly reduced by administration of metformin or SR-18292 (Fig. 5). Evaluation of tumors using a caliper and conventional volume calculation provided overlapping results (data not shown). No differences in liver/body weight ratio and lung/body weight ratio were observed (Fig. S7). These data show that interference with mitochondrial respiration or PGC-1α selectively modulates the growth of tumors derived from stem cell-enriched cultures.

Based on the results described above, we next focused on the effects of metformin and SR-18292 on the molecular characteristic of tumors derived from SPH. The weight of tumors and the number of proliferating cells, as assessed by BrdU immunostaining, were significantly reduced by treatment with both drugs (Fig. 6A-B). Gene expression profiles derived from a PCR array specific for liver cancer pathways revealed common downregulated genes in tumors from mice injected with SPH and treated with metformin or SR-18292 (Fig. 6C). These included markers of apoptosis (*i.e.* BIRC2, CFLAR, GSTP1, BID) and cell cycle (CCND1, GADD45B, EP300, PTEN) as well as genes involved in signal transduction such as the Wnt pathway, MAP kinase or Met signaling, and DNA damage and repair (*i.e.* MSH2, XIAP). Tumor tissues belonging to mice treated with SR-18292 showed a peculiar set of downregulated genes which contained more cell cycle-related genes, together with genes involved in immune and inflammatory responses or angiogenesis. Of note, gene cluster analysis showed that tumors from mice injected with SPH and treated with metformin or SR-18292 were more similar to those derived from MON than to those of untreated mice injected with SPH. At the protein level, suppression of PGC-1α was associated with an increase in HKII expression, suggesting a metabolic shift towards a more glycolytic-like phenotype (Fig. 6D). Moreover, treatment with SR-18292 had an impact on AKT activation, EMT and angiogenesis (CD31), thus confirming the PCR array data. In aggregate, these findings indicate an OXPHOS-addicted phenotype of the CCA-stem-like component and suggest that CCA CSCs adapt to stress conditions by acquiring mitochondrial flexibility, which is functionally relevant for the maintenance of a stem-like phenotype.

Genes related to the mitochondrial system predict poor prognosis in CCA patients

To translate our *in vitro* data to the clinical setting, we exploited a published cohort of patients with CCA[29], who were dichotomically stratified into 'poor' survival (<12 months, 30 patients) and 'good' survival (>12 months, 64 patients) (Fig. 7A). Both

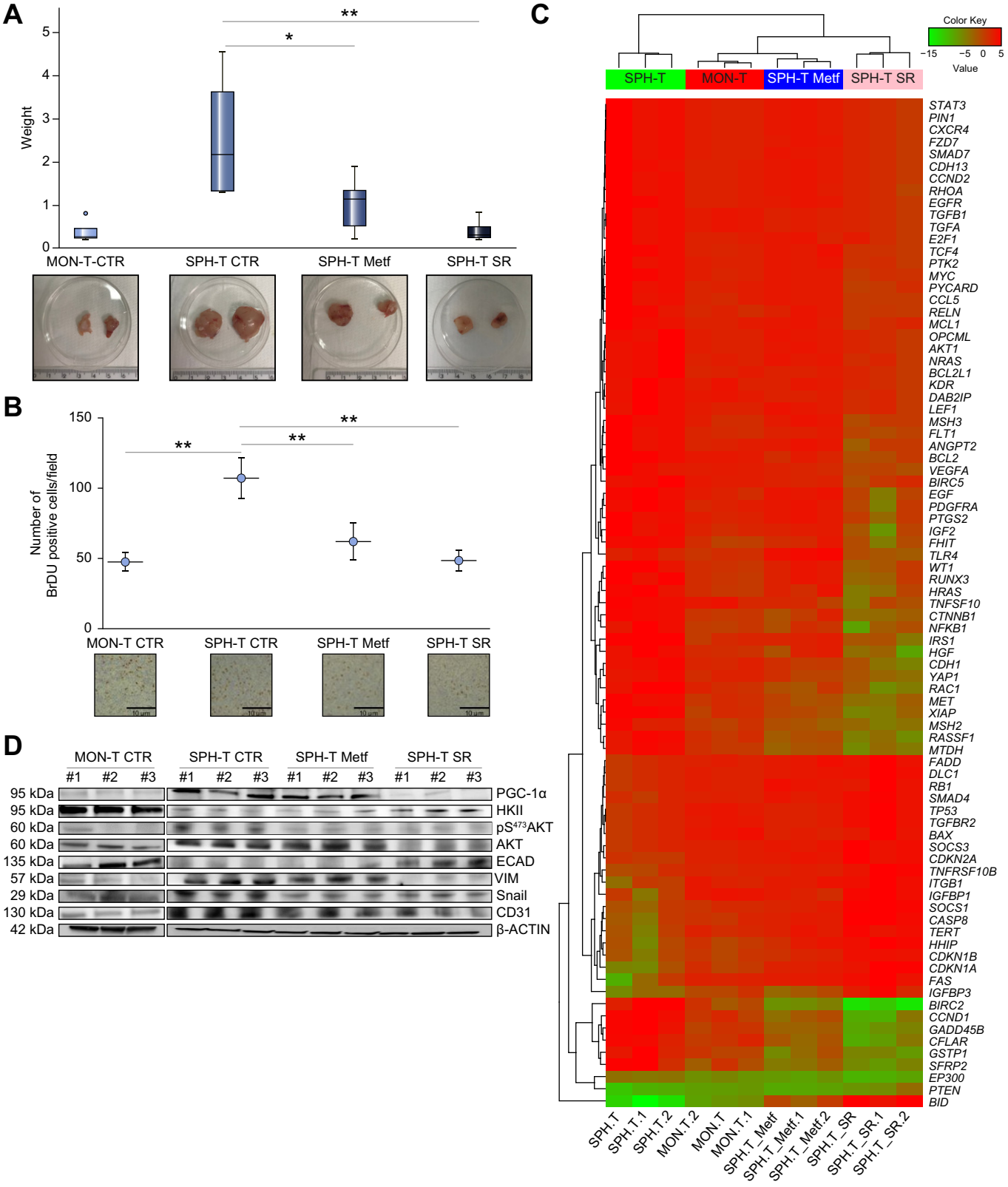

Fig. 6. Phenotypic characteristic of CCA SPH xenografts following treatment with metformin or SR-18292 or in comparison to MON-derived tumors. (A) Tumor weight, depicted as in Fig. 5A. Representative dissected tumor samples are shown below the box-plot. $^{**}p \leq 0.002$, $^{*}p = 0.016$ by two-tailed unpaired *t* test. (B) BrdU incorporation by immunostaining assay. Mean ± SEM ($^{**}p \leq 0.01$ by Student's *t* test). Representative stainings are shown below the barogram, BrdU-positive nuclei are in brown color. Scale bar 10 μm. (C) qRT-PCR arrays focused on liver cancer pathways. Heatmap of different tumor samples based on expression of 84 genes. Gene expression levels are expressed in color code from green (low) to red (high) according to the color key scale bar. Hierarchical clustering was based on complete linkage on euclidean distances between genes (rows) or samples (columns). (D) Immunoblot of different proteins and phosphoproteins in tumor samples from different groups. CCA, cholangiocarcinoma; MON, monolayer cultures; qRT-PCR, quantitative reverse-transcription PCR; SPH, sphere cultures; MON-T, tumors derived from injected monolayer cells; SPH-T,tumors derived from injected sphere cells.

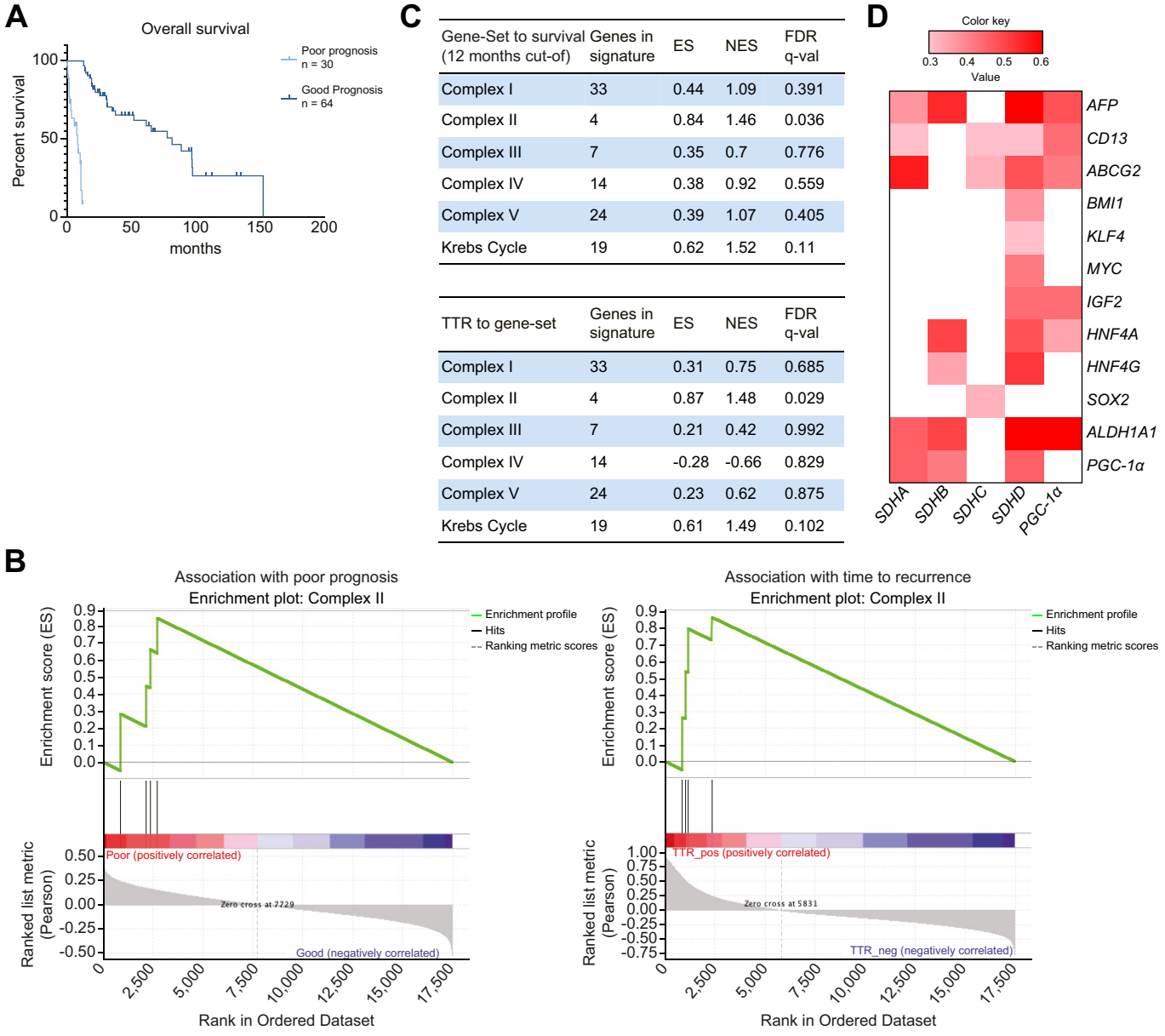

Gene-Set to survival (12 months cut-of)	Genes in signature	ES	NES	FDR q-val
Complex I	33	0.44	1.09	0.391
Complex II	4	0.84	1.46	0.036
Complex III	7	0.35	0.7	0.776
Complex IV	14	0.38	0.92	0.559
Complex V	24	0.39	1.07	0.405
Krebs Cycle	19	0.62	1.52	0.11

TTR to gene-set	Genes in signature	ES	NES	FDR q-val
Complex I	33	0.31	0.75	0.685
Complex II	4	0.87	1.48	0.029
Complex III	7	0.21	0.42	0.992
Complex IV	14	-0.28	-0.66	0.829
Complex V	24	0.23	0.62	0.875
Krebs Cycle	19	0.61	1.49	0.102

Fig. 7. Expression of respiratory complex II is associated with poor survival and recurrence in patients with CCA. (A). Kaplan-Meyer plot showing overall survival in 94 iCCA patients stratified according to good or bad prognosis. (B) GSEA of custom gene sets representing respiratory complex I-V and Krebs cycle. (C) Number of genes in signature, ES and NES reflect positive or negative association with a trait with FDR-corrected q-value. Enrichment plots show significantly associated respiratory complex II signature with patient outcomes. (D) Correlation between expression of complex II (SDHA, SDHB, SDHC, SDHD) or PGC-1α genes (x-axis) and stem-like genes (y-axis) in a published microrarray-based study comparing CCA *vs.* surrounding liver (GSE26566[25]). All adjusted (2-tailed) *p* values were <1e-5. CCA, cholangiocarcinoma; ES, enrichment score; FDR, false discovery rate; GSEA, gene set-enrichment analysis; NES, normalized enrichment score; SPH, sphere cultures.

groups were tested for enhanced expression of crucial mitochondrial enzymes involved in the electron transport chain (complex I-V) as well as in the Krebs cycle, by GSEA. Interestingly, expression of genes of complex II (SDHA, SDHB, SDHC, SDHD) significantly correlated with overall survival (p = 0.036), whereas the other gene sets did not reach statistical significance (Fig. 7B). Moreover, expression of complex II genes predicted a shorter time to recurrence (p = 0.029, Fig. 7C). Accordingly, a substantial correlation between PGC-1α, complex II and genes related to stemness was observed in patients with CCA (Fig. 7D, Table S1).

We next investigated PGC-1α expression at the protein level by immunohistochemistry in a different cohort, observing variable degrees of expression (Fig. 8A). Notably, patients with a high PGC-1α immunostaining score had shorter overall and progression-free survival, and higher angioinvasion and recurrence

compared to patients with a low PGC-1α score (Fig. 8B-E). These data further indicate that in patients with CCA, PGC-1 α expression is associated with significantly worse clinical outcomes.

Discussion

CSCs are endowed with self-renewal, pluripotency, plasticity and differentiation potential. Due to these characteristics, they play a pivotal role in initiation, progression, and response to treatment in many types of cancer. Recent investigations have highlighted the concept that cancer is characterized by specific metabolic features, whereby genetic and environmental variables may be accompanied by acquisition of a different metabolic state. In spite of the significance of CSCs in cancer and of the limited therapeutic opportunities available in CCA, the metabolic characteristics of CSCs and their potential relevance in the biology of this tumor have not been explored.

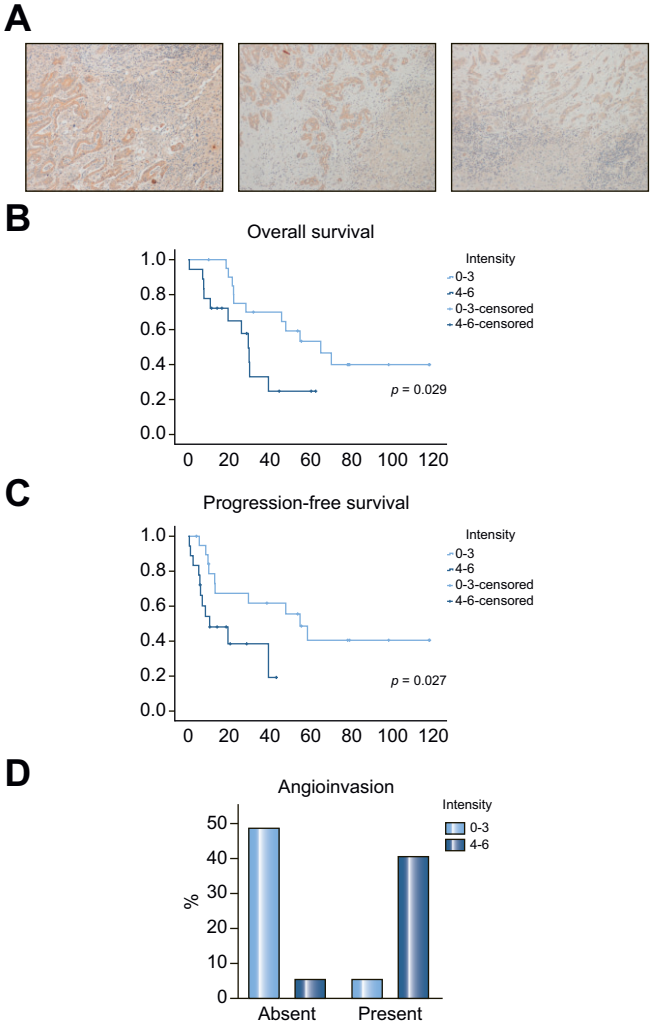

Fig. 8. Staining for PGC-1α correlates with clinical characteristics of CCA. (A) Immunostaining for PCG-1α in 3 representative CCA specimens. Homogeneous and strong staining in cancer cells (upper panel); moderate cytoplasmic immunoreactivity (middle panel); faint cytoplasmic immunoreactivity (lower panel). Original magnification 20x, scale bar 10 μM. (B) Kaplan-Meier survival curves for patients grouped according to staining intensity. (C). Kaplan-Meier progression-free survival curves for the same groups as in (B). (D) Presence of angioinvasion in for patients grouped according to staining intensity (Fisher exact test, p <0.001). CCA, cholangiocarcinoma.

Data reported in this study indicate that in CCA, stem-like cells undergo metabolic reprogramming, resulting in a potentiated OXPHOS system, while cells grown in MON, a condition not associated with stemness features, rely more on glycolysis to meet their energy demands. Mitochondrial respiration is far more efficient in energy production than glycolysis, generating 36 molecules of ATP per molecule of glucose, as opposed to only 2 molecules of ATP produced in glycolysis. In agreement with metabolic data, CCA CSCs showed marked changes in the number of mitochondria, and in their membrane potential. These changes are likely to be very relevant when considering that one of the most striking characteristics of CSCs is their ability to form a specialized niche, termed the CSC microenvironment,[21] to adapt to changing conditions.[10,20] This specific milieu facilitates tumor progression by maintaining the principal properties of CSCs. Indeed, CSCs are characterized by a highly plastic metabolism, which allows them to survive under conditions of metabolic stress by readily switching between OXPHOS and glycolysis. These changes are to some extent tumor cell-specific.[32] CCA is exquisitely sensitive to a specific microenvironment, which is characterized by a thick fibrillar stroma where oxygen and nutrients may be scarce. Based on the results of this study, the acquisition of a more efficient oxidative metabolism may allow CCA stem-like cells to better survive in these conditions. Accordingly, the machinery for efficient glycolysis was more developed in MON than in SPH, compatible with the leading role of OXPHOS in the latter culture condition. These data lead us to speculate that, in CCA, metabolic rewiring to OXPHOS renders CSCs resistant to inhibition of glycolysis, providing the cells with a higher degree of independence from microenvironmental nutrient supply.

Mitochondria play a pivotal role in regulating respiration, and the observed changes in their number and function are clearly related to data on OXPHOS. More important, we demonstrated that these changes in metabolism had a functional role. We first analyzed the effects of metformin and phenformin, both well-established inhibitors of mitochondrial respiration complex I. SPH exposed to these drugs showed a dose-dependent reduction in cell survival, and a profound modulation of the expression of different genes implicated in the biology of CCA, an effect absent in MON, where mitochondrial respiration appears to be less essential. Specifically, genes related to stemness and to angiogenesis were significantly less expressed, while markers of epithelial differentiation, *e.g.* E-cadherin, were increased. These effects suggest that the mitochondrial respiration pathway may support the growth and aggressiveness of CCA enriched with a stem-like components.

Although the mechanisms determining the observed OXPHOS phenotype are still unclear, we next aimed to establish a link between regulatory proteins of mitochondrial biogenesis and the stemness properties of CCA cells.[33–37] We focused on the transcription factor PGC-1α, a key regulator of mitochondrial biogenesis, which enhances oxidative phosphorylation in many invasive and highly malignant cancer cells.[38–40] This factor was also recently shown to regulate OXPHOS functionality and, most importantly, self-renewal and tumorigenic capacity of pancreatic $CD133^+$ CSCs.[34] In CCA cells, genetic knockdown of PGC-1α decreased CSCs markers, *in vitro* self-renewal potential and invasive capacity of stem-like cells. These results were confirmed and expanded using SR-18292, a specific inhibitor of PGC-1α. In both cell lines used in this study, exposure to SR-18292 reduced

mitochondrial biogenesis and sphere formation. These effects were associated with downregulation of signaling pathways linked to malignancy and EMT, and lower expression of genes related to self-renewal, pluripotency and drug transport. These data support the dependence of stem-like cells on mitochondrial biogenesis and activity and identify an upstream molecular mechanism.

Tumors grow in a tridimensional and multicellular environment, and cell culture is only partially representative of an *in vivo condition.* Thus, we analyzed tumor xenografts developed in mice using CCA cells from MON or SPH cultures, and the effects of treatment with metformin or SR-18292. Remarkably, the effects of these drugs were non-significant in tumors developed after MON injection. In contrast, tumors derived from SPH were larger, and their volume was reduced by inhibiting mitochondrial respiration (with metformin) or PGC-1α expression (with SR-18292). At a molecular level, the gene signature of tumors derived from SPH was characterized by upregulation of several pathways associated with malignancy. In contrast, treatment of mice with metformin or SR-18292 made the signature of SPH-derived tumors more similar to that of tumors derived from MON. Of note, the effects of SR-18292 were not completely overlapping with those of metformin and included upregulation of genes involved in the glycolytic pathway and reduced expression of genes regulating EMT or angiogenesis. Taken together, these data provide for the first time, in CCA, a direct correlation between oxidative metabolism and PGC-1α expression, the phenotype of stem-like cells, and the development of CCA xenografts *in vivo.*

CSCs dynamically shape their microenvironment to maintain a supportive niche, and drive interactions with other tumor components, such as immune cells, cancer-associated fibroblasts, and endothelial cells, to maintain a milieu which favors their survival and growth. This is achieved via a complex crosstalk with other cells of the niche, including secretion of soluble mediators, such as VEGF, which promotes angiogenesis through paracrine signals.[41–47] In CCA-SPH, PGC-1α silencing downregulated the ability of SPH to express VEGF, phenocopying the effects of exposure to metformin. In addition, depletion of PGC-1α reduced the ability of SPH-conditioned medium to induce tube formation, a functional angiogenic assay. Along these lines, acquisition of a mesenchymal phenotype, via a EMT process, is a well-established feature of highly malignant cancers.[48,49] In SPH, PGC-1α and mitochondrial respiration significantly upregulated molecules involved in EMT, which was also upregulated by activation of AMPK. Altogether, these data identify mitochondrial respiration as a new pathway regulated by PGC-1α and responsible for maintenance of a stem-like phenotype and potentially of the angiogenic niche and EMT in CCA.

The ultimate goal of translational research is to identify and validate novel pathways or targets, the interference with which could be eventually investigated in clinical trials. For this strategy to be rational and possibly successful, the targets emerging from cell culture and animal experiments must be present and modulated in biologic material collected from patients with the condition of interest. We first exploited transcriptomic data from a published cohort of patients with CCA to search for possible correlations between factors implicated in mitochondrial biogenesis and respiration, expression of genes involved in the aggressive biology of CCA, and clinical outcomes. In this respect, we found several levels of interaction. Expression of PGC-1α in SPH significantly and directly correlated with different genes implicated in stemness and was strongly and directly correlated with expression of VEGF, supporting the relation between mitochondrial biogenesis and the angiogenic niche. Remarkably, mitochondrial complex II expression correlated with a poor prognosis when patients were dichotomically divided according to their outcome, and the same factor and PGC-1α correlated with several CSC-related genes in an oligoarray heatmap. In a different cohort of patients, high-grade staining for PGC-1α identified a subgroup of patients with shortened overall and progression-free survival.

In conclusion, we have characterized the metabolic features of CSCs from CCA, highlighting the predominance of oxidative metabolism, supported by increased mitochondrial biogenesis and signals generated via PGC-1α. These lines of information provide significant advances in our understanding of the biology of CSCs in CCA that could be of eventual relevance for the management of this deadly tumor.

Abbreviations

CCA, cholangiocarcinoma; CSC(s), cancer stem cells; ECAR, extracellular acidification rate; EMT, epithelial-to-mesenchymal transition; GSEA, gene set-enrichment analysis; HKII, hexokinase II; MON, monolayer cultures; OCR, oxygen consumption rate; OXPHOS, oxidative phosphorylation; PGC-1α, peroxisome proliferator-activated receptor gamma coactivator 1-α; SPH, sphere cultures; VEGF, vascular endothelial growth factor.

Financial support

Funding for this work was partially provided by Associazione Italiana per la Ricerca sul Cancro (AIRC, MFGA17588, IG23117) to Dr. Raggi and (IG17786) to Prof. Marra. Dr. Lori is supported in part by a Fellowship from Fondazione Italiana per la Ricerca sul Cancro (FIRC-AIRC). Financial support from the University of Florence, Fondazione Umberto Veronesi, Italian Ministry of University and Research (MIUR) through grant "Dipartimenti di Eccellenza - 2017" to University of Milano Bicocca, Department of Biotechnology and Biosciences is also acknowledged.

Conflicts of interest

The authors have no conflicts of interest to disclose.

Please refer to the accompanying ICMJE disclosure forms for further details.

Authors' contributions

CR, FM designed the study and wrote the manuscript. MLT, ES, NN, MC, BP, MP, CC, EP, JI, TL, GL, CP, JC, ML, JBA, LDT, LV, GDM, SM, MR, IO, AA, PC provided materials, performed the experiments, collected the data, and analyzed the results. CR, FM supervised the project and critically revised the manuscript. All authors have read and approved the final manuscript.

Data availability statement

The data that support the findings of this study are available from the corresponding authors [FM, CR], upon reasonable request.

Acknowledgments

The authors thank Dr. A.J. Demetris (University of Pittsburgh, Pittsburgh, PA, USA) for cholangiocarcinoma cell lines (HUCCT1

and CCLP1). The authors thank Prof. Betti Giusti (University of Florence, Florence, Italy) for the use of ABI7900HT equipment.

Supplementary data

Supplementary data to this article can be found online at https://doi.org/10.1016/j.jhep.2020.12.031.

References

Author names in bold designate shared co-first authorship

[1] Khan SA, Tavolari S, Brandi G. Cholangiocarcinoma: epidemiology and risk factors. Liver Int 2019;39(Suppl 1):19–31.

[2] Bertuccio P, Malvezzi M, Carioli G, Hashim D, Boffetta P, El-Serag HB, et al. Reply to: "Global trends in mortality from intrahepatic and extrahepatic cholangiocarcinoma". J Hepatol 2019;71:1262–1263.

[3] Banales JM, Marin JJG, Lamarca A, Rodrigues PM, Khan SA, Roberts LR, et al. Cholangiocarcinoma 2020: the next horizon in mechanisms and management. Nat Rev Gastroenterol Hepatol 2020;17:557–588.

[4] Banales JM, Cardinale V, Carpino G, Marzioni M, Andersen JB, Invernizzi P, et al. Expert consensus document: cholangiocarcinoma: current knowledge and future perspectives consensus statement from the European Network for the Study of Cholangiocarcinoma (ENS-CCA). Nat Rev Gastroenterol Hepatol 2016;13:261–280.

[5] Shaib Y, El-Serag HB. The epidemiology of cholangiocarcinoma. Semin Liver Dis 2004;24:115–125.

[6] Yamashita T, Honda M, Nakamoto Y, Baba M, Nio K, Hara Y, et al. Discrete nature of EpCAM+ and CD90+ cancer stem cells in human hepatocellular carcinoma. Hepatology 2013;57:1484–1497.

[7] Oikawa T. Cancer Stem cells and their cellular origins in primary liver and biliary tract cancers. Hepatology 2016;64:645–651.

[8] **Marquardt JU**, **Raggi C**, Andersen JB, Seo D, Avital I, Geller D, et al. Human hepatic cancer stem cells are characterized by common stemness traits and diverse oncogenic pathways. Hepatology 2011;54:1031–1042.

[9] Raggi C, Factor VM, Seo D, Holczbauer A, Gillen MC, Marquardt JU, et al. Epigenetic reprogramming modulates malignant properties of human liver cancer. Hepatology 2014;59:2251–2262.

[10] **Raggi C**, **Mousa HS**, **Correnti M**, Sica A, Invernizzi P. Cancer stem cells and tumor-associated macrophages: a roadmap for multitargeting strategies. Oncogene 2016;35:671–682.

[11] Raggi C, Invernizzi P, Andersen JB. Impact of microenvironment and stem-like plasticity in cholangiocarcinoma: molecular networks and biological concepts. J Hepatol 2015;62:198–207.

[12] Correnti M, Raggi C. Stem-like plasticity and heterogeneity of circulating tumor cells: current status and prospect challenges in liver cancer. Oncotarget 2017;8:7094–7115.

[13] **Raggi C**, **Correnti M**, Sica A, Andersen JB, Cardinale V, Alvaro D, et al. Cholangiocarcinoma stem-like subset shapes tumor-initiating niche by educating associated macrophages. J Hepatol 2017;66:102–115.

[14] **Raggi C**, **Gammella E**, Correnti M, Buratti P, Forti E, Andersen JB, et al. Dysregulation of iron metabolism in cholangiocarcinoma stem-like cells. Sci Rep 2017;7:17667.

[15] Vicent S, Lieshout R, Saborowski A, Verstegen MMA, Raggi C, Recalcati S, et al. Experimental models to unravel the molecular pathogenesis, cell of origin and stem cell properties of cholangiocarcinoma. Liver Int 2019;39(Suppl 1):79–97.

[16] Nevi L, Costantini D, Safarikia S, Di Matteo S, Melandro F, Berloco PB, et al. Cholest-4,6-Dien-3-One promote epithelial-to-mesenchymal transition (EMT) in biliary tree stem/progenitor cell cultures in vitro. Cells 2019;8.

[17] **Carpino G**, **Cardinale V**, Folseraas T, Overi D, Grzyb K, Costantini D, et al. Neoplastic transformation of the peribiliary stem cell niche in cholangiocarcinoma arisen in primary sclerosing cholangitis. Hepatology 2019;69:622–638.

[18] Pant K, Richard S, Peixoto E, Gradilone SA. Role of glucose metabolism reprogramming in the pathogenesis of cholangiocarcinoma. Front Med (Lausanne) 2020;7:113.

[19] Li Dan, Wang C, Ma P, Yu Q, Gu M, Dong L, et al. PGC1α promotes cholangiocarcinoma metastasis by upregulating PDHA1 and MPC1 expression to reverse the Warburg effect. Cell Death Dis 2018;9:466.

[20] Ippolito L, Marini A, Cavallini L, Morandi A, Pietrovito L, Pintus G, et al. Metabolic shift toward oxidative phosphorylation in docetaxel resistant prostate cancer cells. Oncotarget 2016;7:61890–61904.

[21] Taddei ML, Cavallini L, Ramazzotti M, Comito G, Pietrovito L, Morandi A, et al. Stromal-induced downregulation of miR-1247 promotes prostate cancer malignancy. J Cell Physiol 2019;234:8274–8285.

[22] Wu Z, Puigserver P, Andersson U, Zhang C, Adelmant G, Mootha V, et al. Mechanisms controlling mitochondrial biogenesis and respiration through the thermogenic coactivator PGC-1. Cell 1999;98:115–124.

[23] Piccinin E, Peres C, Bellafante E, Ducheix S, Pinto C, Villani G, et al. Hepatic peroxisome proliferator-activated receptor γ coactivator 1β drives mitochondrial and anabolic signatures that contribute to hepatocellular carcinoma progression in mice. Hepatology 2018;67:884–898.

[24] Jäger S, Handschin C, St-Pierre J, Spiegelman BM. AMP-activated protein kinase (AMPK) action in skeletal muscle via direct phosphorylation of PGC-1alpha. Proc Natl Acad Sci U S A 2007;104:12017–12022.

[25] Wang X, Pan X, Song J. AMP-activated protein kinase is required for induction of apoptosis and epithelial-to-mesenchymal transition. Cell Signal 2010;22:1790–1797.

[26] **He K**, **Guo X**, Liu Y, Li J, Hu Y, Wang D, et al. TUFM downregulation induces epithelial-mesenchymal transition and invasion in lung cancer cells via a mechanism involving AMPK-GSK3β signaling. Cell Mol Life Sci 2016;73:2105–2121.

[27] Cantó C, Auwerx J. PGC-1alpha, SIRT1 and AMPK, an energy sensing network that controls energy expenditure. Curr Opin Lipidol 2009;20:98–105.

[28] Liu X, Chhipa RR, Nakano I, Dasgupta B. The AMPK inhibitor compound C is a potent AMPK-independent antiglioma agent. Mol Cancer Ther 2014;13:596–605.

[29] Andersen JB, Spee B, Blechacz BR, Avital I, Komuta M, Barbour A, et al. Genomic and genetic characterization of cholangiocarcinoma identifies therapeutic targets for tyrosine kinase inhibitors. Gastroenterology 2012;142:1021–1031. e1015.

[30] Sharabi K, Lin H, Tavares CDJ, Dominy JE, Camporez JP, Perry RJ, et al. Selective chemical inhibition of PGC-1α gluconeogenic activity ameliorates type 2 diabetes. Cell 2017;169:148–160. e115.

[31] Miller KN, Clark JP, Anderson RM. Mitochondrial regulator PGC-1a-Modulating the modulator. Curr Opin Endocr Metab Res 2019;5:37–44.

[32] Vlashi E, Lagadec C, Vergnes L, Reue K, Frohnen P, Chan M, et al. Metabolic differences in breast cancer stem cells and differentiated progeny. Breast Cancer Res Treat 2014;146:525–534.

[33] **Janiszewska M**, **Suvà ML**, Riggi N, Houtkooper RH, Auwerx J, Clément-Schatlo V, et al. Imp2 controls oxidative phosphorylation and is crucial for preserving glioblastoma cancer stem cells. Genes Dev 2012;26:1926–1944.

[34] Sancho P, Burgos-Ramos E, Tavera A, Bou Kheir T, Jagust P, Schoenhals M, et al. MYC/PGC-1α balance determines the metabolic phenotype and plasticity of pancreatic cancer stem cells. Cell Metab 2015;22:590–605.

[35] **De Luca A**, **Fiorillo M**, Peiris-Pagès M, Ozsvari B, Smith DL, Sanchez-Alvarez R, et al. Mitochondrial biogenesis is required for the anchorage-independent survival and propagation of stem-like cancer cells. Oncotarget 2015;6:14777–14795.

[36] **Pastò A**, **Bellio C**, **Pilotto G**, Ciminale V, Silic-Benussi M, Guzzo G, et al. Cancer stem cells from epithelial ovarian cancer patients privilege oxidative phosphorylation, and resist glucose deprivation. Oncotarget 2014;5:4305–4319.

[37] Lamb R, Harrison H, Hulit J, Smith DL, Lisanti MP, Sotgia F. Mitochondria as new therapeutic targets for eradicating cancer stem cells: quantitative proteomics and functional validation via MCT1/2 inhibition. Oncotarget 2014;5:11029–11037.

[38] LeBleu VS, O'Connell JT, Gonzalez Herrera KN, Wikman H, Pantel K, Haigis MC, et al. PGC-1α mediates mitochondrial biogenesis and oxidative phosphorylation in cancer cells to promote metastasis. Nat Cell Biol 2014;16:992–1003. 1001-1015.

[39] Cheong H, Lu C, Lindsten T, Thompson CB. Therapeutic targets in cancer cell metabolism and autophagy. Nat Biotechnol 2012;30:671–678.

[40] **Li Y**, **Xu S**, Li J, Zheng L, Feng M, Wang X, et al. SIRT1 facilitates hepatocellular carcinoma metastasis by promoting PGC-1α-mediated mitochondrial biogenesis. Oncotarget 2016;7:29255–29274.

[41] Conley SJ, Gheordunescu E, Kakarala P, Newman B, Korkaya H, Heath AN, et al. Antiangiogenic agents increase breast cancer stem cells via the generation of tumor hypoxia. Proc Natl Acad Sci U S A 2012;109:2784–2789.

[42] **Hasmim M**, **Noman MZ**, Messai Y, Bordereaux D, Gros G, Baud V, et al. Cutting edge: hypoxia-induced Nanog favors the intratumoral infiltration of regulatory T cells and macrophages via direct regulation of TGF-β1. J Immunol 2013;191:5802–5806.

[43] Maxwell PH, Dachs GU, Gleadle JM, Nicholls LG, Harris AL, Stratford IJ, et al. Hypoxia-inducible factor-1 modulates gene expression in solid tumors and influences both angiogenesis and tumor growth. Proc Natl Acad Sci U S A 1997;94:8104–8109.
[44] Bao S, Wu Q, Sathornsumetee S, Hao Y, Li Z, Hjelmeland AB, et al. Stem cell-like glioma cells promote tumor angiogenesis through vascular endothelial growth factor. Cancer Res 2006;66:7843–7848.
[45] Flavahan WA, Wu Q, Hitomi M, Rahim N, Kim Y, Sloan AE, et al. Brain tumor initiating cells adapt to restricted nutrition through preferential glucose uptake. Nat Neurosci 2013;16:1373–1382.
[46] Carcereri de Prati A, Butturini E, Rigo A, Oppici E, Rossin M, Boriero D, et al. Metastatic breast cancer cells enter into dormant state and express cancer stem cells phenotype under chronic hypoxia. J Cell Biochem 2017;118:3237–3248.
[47] Siebzehnrubl FA, Silver DJ, Tugertimur B, Deleyrolle LP, Siebzehnrubl D, Sarkisian MR, et al. The ZEB1 pathway links glioblastoma initiation, invasion and chemoresistance. EMBO Mol Med 2013;5:1196–1212.
[48] Gooding AJ, Schiemann WP. Epithelial-mesenchymal transition programs and cancer stem cell phenotypes: mediators of breast cancer therapy resistance. Mol Cancer Res 2020;18:1257–1270.
[49] Yang J, Antin P, Berx G, Blanpain C, Brabletz T, Bronner M, et al. Guidelines and definitions for research on epithelial-mesenchymal transition. Nat Rev Mol Cell Biol 2020;21:341–352.